
Relative-Translation Invariant Wasserstein Distance

Binshuai Wang¹, Qiwei Di², Ming Yin³, Mengdi Wang³, Quanquan Gu² and Peng Wei¹

¹Computer Science Department, George Washington University
{derekwang, pwei}@gwu.edu

²Computer Science Department, University of California, Los Angeles
{qiwei2000, qgu}@cs.ucla.edu

³Electrical and Computer Engineering Department, Princeton University
{my0049, mengdiw}@princeton.edu

Abstract

We introduce a new family of distances, relative-translation invariant Wasserstein distances (RW_p), for measuring the similarity of two probability distributions under distribution shift. Generalizing it from the classical optimal transport model, we show that RW_p distances are also real distance metrics defined on the quotient set $\mathcal{P}_p(\mathbb{R}^n)/\sim$ and invariant to distribution translations. When $p = 2$, the RW_2 distance enjoys more exciting properties, including decomposability of the optimal transport model, translation-invariance of the RW_2 distance, and a Pythagorean relationship between RW_2 and the classical quadratic Wasserstein distance (W_2). Based on these properties, we show that a distribution shift, measured by W_2 distance, can be explained in the bias-variance perspective. In addition, we propose a variant of the Sinkhorn algorithm, named RW_2 Sinkhorn algorithm, for efficiently calculating RW_2 distance, coupling solutions, as well as W_2 distance. We also provide the analysis of numerical stability and time complexity for the proposed algorithm. Finally, we validate the RW_2 distance metric and the algorithm performance with three experiments. We conduct one numerical validation for the RW_2 Sinkhorn algorithm and show two real-world applications demonstrating the effectiveness of using RW_2 under distribution shift: digits recognition and similar thunderstorm detection. The experimental results report that our proposed algorithm significantly improves the computational efficiency of Sinkhorn in certain practical applications, and the RW_2 distance is robust to distribution translations compared with baselines.

1 Introduction

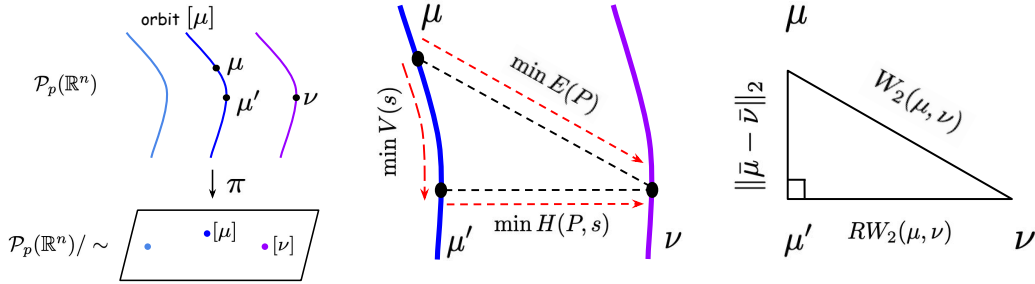
Optimal transport (OT) theory and Wasserstein distance [Peyré and Cuturi, 2020, Janati et al., 2020, Villani, 2009] provide a rigorous measurement of similarity between two probability distributions. Numerous state-of-the-art machine learning applications are developed based on the OT formulation and Wasserstein distances, including domain adaptation, score-based generative model, Wasserstein generative adversarial networks, Fréchet inception distance (FID) score, Wasserstein auto-encoders, distributionally robust Markov decision processes, distributionally robust regressions, graph neural networks based objects tracking, etc [Shen et al., 2017, Pinheiro, 2017, Courty et al., 2017b, Damodaran et al., 2018, Courty et al., 2017a, Arjovsky et al., 2017, Heusel et al., 2017, Tolstikhin et al., 2017, Clement and Kroer, 2021, Shafieezadeh-Abadeh et al., 2015, Chen and Paschalidis, 2018, Yu et al., 2023, Sarlin et al., 2019]. However, the classical Wasserstein distance has major limitations in certain machine learning and computer vision applications. For example, a meteorologist often focuses on identifying similar weather patterns in a large-scale geographical region Wang et al. [2023], Roberts and Lean [2008], Dixon and Wiener [1993], where he/she cares more about the “shapes” of weather events rather than their exact locations. The weather events are represented as images or point

clouds from the radar reflectivity map. Here the classical Wasserstein distance is not useful since the relative location difference or relative translation between two very similar weather patterns will add to the Wasserstein distance value. Another example is the inevitable distribution shift in real-world datasets. A distribution shift may be introduced by sensor calibration error, environment changes between train and test datasets, simulation to real-world (*sim2real*) deployment, etc. Motivated by these practical use cases and the limitations of Wasserstein distances, we ask the following research question:

Can we find a new distance metric and a corresponding efficient algorithm to measure the similarity between probability distributions (and their supports) regardless of their relative translation?

To answer this research question, we introduce the relative translation optimal transport (ROT) problem and the corresponding relative-translation invariant Wasserstein distance RW_p . We then focus on the quadratic case ($p = 2$) and identify three exciting properties of the RW_2 distance. We leverage these properties to design a variant of the Sinkhorn algorithm to compute RW_2 distance, coupling solutions, as well as W_2 distance. In addition, we provide analysis and numerical experiment results to demonstrate the effectiveness of the new RW_2 distance against translation shifts. Finally, we show the scalability and practical usage of the RW_2 in a real-world meteorological application.

Contributions. The main contributions of this paper are highlighted as follows: (a) we introduce a family of new similarity metrics, relative-translation invariant Wasserstein (RW_p) distances, which are real distance metrics like the Wasserstein distance and invariant to the relative translation of two distributions; (b) we identify three useful properties of the quadratic case RW_2 to support our algorithm design: decomposability of the ROT problem, translation-invariance of both the ROT problem solution and the resulted RW_2 , and Pythagorean relationship between RW_2 and the classical W_2 ; (c) we show that the RW_2 can be used to analyze and explain a general distribution shift (measured by W_2) in the bias-variance perspective; and (d) we propose an efficient variant of Sinkhorn algorithm, named the RW_2 Sinkhorn, for calculating RW_2 distance, coupling solutions as well as W_2 distance with significantly reduced computational complexity and enhanced numerical stability under relative translations. Empirically, we report promising performance from the proposed RW_2 distance when the relative translation is large, and the RW_2 Sinkhorn algorithm in illustrative numerical examples and a large-scale real-world task for similar weather detection. Figure 1 shows our major findings in this work.



(a) Schematic illustration of the quotient set $\mathcal{P}_p(\mathbb{R}^n)/\sim$, where π stands for the natural projection from $\mathcal{P}_p(\mathbb{R}^n)$ to $\mathcal{P}_p(\mathbb{R}^n)/\sim$. The equivalence class (orbit) $[\mu]$ is pictured as the blue line of μ and μ' in $\mathcal{P}_p(\mathbb{R}^n)$ and it corresponds to a point $[\mu]$ in the quotient set $\mathcal{P}_p(\mathbb{R}^n)/\sim$.
 (b) Decomposition of the optimal transport optimization. To move μ distances, μ can be moved along the orbit (equivalence class) $[\mu]$ to μ' first, which is related to the vertical optimization $V(s)$, then moved on the quotient set $\mathcal{P}_p(\mathbb{R}^n)/\sim$ to the target ν , which is related to the horizontal optimization $H(P, s)$.
 (c) Pythagorean relationship of the three objective functions, $E(P)$, $H(P, s)$ and $V(s)$, respectively, as shown in the sub-figure (b).

Figure 1: The relative translation optimal transport problem and RW_p distances.

Notations. Assume that $\mathcal{P}_p(\mathbb{R}^n)$ is the set of all probability distributions with *finite* moments of order p defined on the space \mathbb{R}^n and $\mathcal{M}(\mathbb{R}^n)$ is the set of all probability distributions with *finite* supports defined on the space \mathbb{R}^n . $\mathbb{R}_*^{m_1 \times m_2}$ represents the set of all $m_1 \times m_2$ matrices with non-negative entries. $[\mu]$ represents the equivalence class (orbit) of μ under the shift equivalence relation

in $\mathcal{P}_p(\mathbb{R}^n)$. $\bar{\mu}$ represents the mean of probability distribution μ (data points). \mathbf{e}_m denotes a vector in \mathbb{R}^m where all elements are ones. $\cdot /$ represents the component-wise division.

Related work. Optimal transport theory is a classical area of mathematics with strong connections to probability theory, diffusion processes and PDEs. Due to the vast literature, we refer readers to [Villani and Society, 2003, Ambrosio et al., 2005, Villani, 2009, Oll, 2014] for comprehensive reviews. Computational OT methods have been widely explored, including Greenkhorn algorithm [Altschuler et al., 2017], Network Simplex method [Peyré and Cuturi, 2020], Wasserstein gradient flow [Mokrov et al., 2021, Fan et al., 2022], neural network approximation [Chen and Wang, 2023]. Significant research has also been conducted on Wasserstein distances, such as the sliced Wasserstein distance [Nguyen and Ho, 2023, Mahey et al., 2023, Nguyen and Ho, 2022], Gromov-Wasserstein distance [Sejourne et al., 2021, Le et al., 2022, Alvarez-Melis et al., 2019], etc. Other important topics include Wasserstein barycenter [Guo et al., 2020, Vaskevicius and Chizat, 2023, Korotin et al., 2022, Lin et al., 2020, Korotin et al., 2021] and unbalanced optimal transport [Nguyen et al., 2024, Chizat, 2017].

2 Preliminaries

Before delving into the details of our proposed method, it is essential to focus on the groundwork with an introduction to key aspects of classical optimal transport theory and formulations. This foundation will support the subsequent derivations and proofs presented in Section 3.

2.1 Optimal Transport Theory

The optimal transport theory focuses on finding the minimal-cost transport plans for moving one probability distribution to another probability distribution in a metric space. The core of this theory involves a cost function, denoted as $c(x, y)$, alongside two probability distributions, $\mu(x)$ and $\nu(y)$. The optimal transport problem is to find the transport plans (coupling solutions) that minimize the cost of moving the distribution $\mu(x)$ to $\nu(y)$, under the cost function $c(x, y)$. Although the cost function can take any non-negative form, our focus will be on those derived from the p -norm, expressed as $\|x - y\|_p^p$ for $p \geq 1$, because the optimal transport problem is well-defined [Villani, 2009].

Assuming $\mu(x)$ as the source distribution and $\nu(y)$ as the target distribution, $\mu, \nu \in \mathcal{P}_p(\mathbb{R}^n)$, we can formulate the optimal transport problem as a functional optimization problem, detailed below:

Definition 1 (p -norm optimal transport problem [Villani, 2009]).

$$OT(\mu, \nu, p) = \min_{\gamma \in \Gamma(\mu, \nu)} \int_{\mathbb{R}^n} \|x - y\|_p^p d\gamma(x, y), \quad (1)$$

with $\Gamma(\mu, \nu) = \{\gamma \in \mathcal{P}_p(\mathbb{R}^n \times \mathbb{R}^n) \mid \int_{\mathbb{R}^n} \gamma(x, y) dx = \nu(y), \int_{\mathbb{R}^n} \gamma(x, y) dy = \mu(x), \gamma(x, y) \geq 0\}$.

Here $\gamma(x, y)$ represents the transport plan (or the coupling solution), indicating the amount of probability mass transported from source support x to target support y . The objective function is to minimize the total transport cost, which is the integrated product cost of distance and transported mass across all source-target pairs (x, y) .

After the foundational optimal transport problem is outlined, we can introduce a family of real metrics, the Wasserstein distances, for measuring the distance between probability distributions on the set $\mathcal{P}_p(\mathbb{R}^n)$. These distances are defined based on the optimal transport problem.

Definition 2 (Wasserstein distances [Villani, 2009]). *The Wasserstein distance between μ and ν is the p th root of the minimal total transport cost from μ to ν , denoted as W_p , ($p \geq 1$):*

$$W_p(\mu, \nu) = OT(\mu, \nu, p)^{\frac{1}{p}}. \quad (2)$$

The Wasserstein distance is a powerful tool for assessing the similarity between probability distributions. It is a real metric admitting the properties of indiscernibility, non-negativity, symmetry, and triangle inequality Villani [2009]. Meanwhile, it is well-defined for any probability distribution pairs, including discrete-discrete, discrete-continuous, and continuous-continuous.

For practical machine learning applications, the functional optimization described in Equation (1) can be adapted into a discrete optimization framework. This adaptation involves considering the distributions, μ and ν , as comprised of *finite* supports, $\{x_i\}_{i=1}^{m_1}$ and $\{y_j\}_{j=1}^{m_2}$, with corresponding probability masses $\{a_i\}_{i=1}^{m_1}$ and $\{b_j\}_{j=1}^{m_2}$, respectively, where m_1 and m_2 are the number of supports

(data points). Since all m_1 and m_2 are finite numbers, we can use an $m_1 \times m_2$ matrix C to represent the cost between supports, where each entry represents the transporting cost from x_i to y_j , i.e., $C_{ij} = \|x_i - y_j\|_p^p$. This discrete version of the optimal transport problem can then be expressed as a linear programming problem, denoted as $\text{OT}(\mu, \nu, p)$:

$$\text{OT}(\mu, \nu, p) = \min_{P_{ij} \in \Pi(\mu, \nu)} \sum_{i=1}^{m_1} \sum_{j=1}^{m_2} C_{ij} P_{ij}, \quad (3)$$

with $\Pi(\mu, \nu) = \{P \in \mathbb{R}_*^{m_1 \times m_2} | P \mathbf{e}_{m_1} = a, P^\top \mathbf{e}_{m_2} = b\}$, where $\Pi(\mu, \nu)$ is the feasible set of this problem, vectors a and b are the probability masses of μ and ν , respectively. coupling solutions P_{ij} indicates the amount of probability mass transported from the source point x_i to the target point y_j . This linear programming approach provides a scalable and efficient way for solving discrete optimal transport problems in various data-driven applications.

2.2 Sinkhorn Algorithm

Equation (3) formulates a linear programming problem, which is commonly solved by simplex methods or interior-point methods Peyré and Cuturi [2020]. Because of the special structure of the feasible set $\Pi(\mu, \nu)$, another approach for solving this problem is to transform it into a matrix scaling problem by adding an entropy regularization in the objective function Cuturi [2013]. The matrix scaling problem can be solved by the Sinkhorn algorithm, which is an iterative algorithm that enjoys both efficiency and scalability. In detail, the Sinkhorn algorithm will initially assign $u^{(0)}$ and $v^{(0)}$ with vector \mathbf{e}_{m_1} and \mathbf{e}_{m_2} , then the vector $u^{(k)}$ and $v^{(k)}$ ($k \geq 1$) are updated alternatively by the following equations:

$$u^{(k+1)} \leftarrow a./Kv^{(k)}, \quad v^{(k+1)} \leftarrow b./K^\top u^{(k+1)}, \quad (4)$$

where $K_{ij} = e^{-\frac{C_{ij}}{\lambda}}$ (λ is the coefficient of the entropy regularized term) and the division is component-wise. When the convergence precision is satisfied, the coupling solution P will be calculated by the matrix $\text{diag}(u)K\text{diag}(v)$. It has been proved the solution calculated by the Sinkhorn algorithm can converge to the exact coupling solution of the linear programming model, as λ goes to zero [Cominetti and Martín, 1994]. One caveat of this calculation is the exponent operation, which may cause ‘‘division by zero’’, we will show how we can improve the numerical stability in Section 4.

3 Relative Translation Optimal Transport and RW_p Distances

Here we present the relative translation optimal transport model and the RW_p distances. We first introduce the general case of the relative translation optimal transport problem and the RW_p distances. We will then focus on the quadratic RW_2 case and its properties.

3.1 Relative Translation Optimal Transport (ROT) Formulation and RW_p Distances

As discussed in Section 1, the classical optimal transport (OT) problem is not useful when there is a relative translation between two distributions (or the two datasets known as their supports). We introduce the *relative translation optimal transport* problem, $\text{ROT}(\mu, \nu, p)$, which is formulated to find the minimal total transport cost under any translation.

Definition 3 (Relative translation optimal transport problem). *Continuing with the previous notations,*

$$\text{ROT}(\mu, \nu, p) = \inf_{s \in \mathbb{R}^n} \min_{P \in \Pi(\mu, \nu)} \sum_{i=1}^{m_1} \sum_{j=1}^{m_2} \|x_i + s - y_j\|_p^p P_{ij}, \quad (5)$$

where variable s represents the translation of source distribution μ , and variables P_{ij} represent the coupling solution between the support x_i and the support y_j .

The ROT problem can be viewed as a generalized form of the classical OT in Equation (1). Different from the one-stage optimization in the classical OT problem, there are two stages in this optimization. The inner optimization is exactly the classical OT, whereas the outer optimization finds the best relative translation for the source distribution to minimize the total transport cost.

Theorem 1 (Compactness and existence of the minimizer). *For Equation (5), the domain of the variable s can be confined to a compact set $\{s \in \mathbb{R}^n | \|s\|_p \leq 2 \max_{ij} \|x_i - y_j\|_p\}$. Thus, we have*

$$\text{ROT}(\mu, \nu, p) = \min_{s \in \mathbb{R}^n} \min_{P \in \Pi(\mu, \nu)} \sum_{i=1}^{m_1} \sum_{j=1}^{m_2} \|x_i + s - y_j\|_p^p P_{ij},$$

where the minimum can be achieved.

The proof of Theorem 1 is provided in Appendix A.

From the perspective of group theory, we could have a better view of which space the ROT problem is defined on. Assume that \sim is the translation relation on the set $\mathcal{P}_p(\mathbb{R}^n)$. When distribution μ can be translated to distribution μ' , we denote it by $\mu \sim \mu'$. Because the translation is an equivalence relation defined on the set $\mathcal{P}_p(\mathbb{R}^n)$, we may divide set $\mathcal{P}_p(\mathbb{R}^n)$ by the translation relation, which leads to a quotient set, $\mathcal{P}_p(\mathbb{R}^n)/\sim$. $\mathcal{P}_p(\mathbb{R}^n)/\sim$ consists of the equivalence class of distributions, and each equivalence class, denoted by $[\mu]$, contains all mutually translatable probability distributions. Therefore, the ROT problem can also be regarded as an OT problem defined on the quotient set, $\mathcal{P}_p(\mathbb{R}^n)/\sim$, which tries to find the minimal total transport cost between $[\mu]$ and $[\nu]$. Figure 1(a) illustrates this idea. We can see that the value of the ROT problem is invariant to translations. This is because the ROT problem is only associated with the equivalence classes of probability distributions.

Building upon the ROT model, we introduce a new family of Wasserstein distances to measure the minimal total transport cost between different equivalence classes of probability distributions. As mentioned above, the value of the ROT problem is invariant to any relative translations, thus, we name the corresponding Wasserstein distances as relative-translation invariant Wasserstein distances, denoted by RW_p , ($p \geq 1$):

Definition 4 (Relative-translation invariant Wasserstein distances).

$$RW_p(\mu, \nu) = ROT(\mu, \nu, p)^{\frac{1}{p}}.$$

Similar to the situation where W_p is a real metric on $\mathcal{P}_p(\mathbb{R}^n)$, we can obtain the following theorem.

Theorem 2. RW_p is a real metric on the quotient set $\mathcal{P}_p(\mathbb{R}^n)/\sim$.

The proof of Theorem 2 is provided in Appendix A. The RW_p can also be regarded as a pseudo-metric defined on the $\mathcal{P}_p(\mathbb{R}^n)$, where the indiscernibility is no longer admitted.

It should be noted that we can not incorporate rotation in our equation 5 since rotation will violate the metric properties and convexity.

3.2 Quadratic ROT and Properties of the RW_2 Distance

We show three useful properties in the quadratic case of ROT and the resulted RW_2 distance: decomposability of the ROT optimization model (Theorem 3), translation-invariance of coupling solutions of the ROT problem (Corollary 1), and Pythagorean relationship of RW_2 and W_2 (Corollary 2). Decomposability will motivate our algorithm design for efficiently solving an ROT problem, translation-invariance provides RW_2 the robustness against distribution shift, and the Pythagorean relationship helps us better understand a distribution shift in the perspective of bias-variance.

Theorem 3 (Decomposition of the quadratic ROT). *Continuing with previous notations, the two-stage optimization problem in quadratic ROT can be decomposed into two independent single-stage optimization problems:*

$$ROT(\mu, \nu, 2) = \min_{s \in \mathbb{R}^n} \min_{P \in \Pi(\mu, \nu)} H(P, s) = \min_{P \in \Pi(\mu, \nu)} (E(P)) + \min_{s \in \mathbb{R}^n} (V(s)) \quad (6)$$

where horizontal function $H(P, s)$ is described by $H(P, s) = \sum_{i=1}^{m_1} \sum_{j=1}^{m_2} \|x_i + s - y_j\|_2^2 P_{ij}$, the overall function $E(P)$ is described by, $E(P) = \sum_{i=1}^{m_1} \sum_{j=1}^{m_2} \|x_i - y_j\|_2^2 P_{ij}$, and vertical function $V(s)$ is described by, $V(s) = \|s\|_2^2 + 2s \cdot (\bar{\mu} - \bar{\nu})$. Moreover, the variables P_{ij} are fully determined by $\min_{P \in \Pi(\mu, \nu)} E(P)$, which is the classical optimal transport problem between μ and ν ; and the variable s is fully determined by $\min_{s \in \mathbb{R}^n} V(s)$, which is a minimization problem of a quadratic function in \mathbb{R}^n and the minimum is achieved when $s = \bar{\nu} - \bar{\mu}$.

Function $E(P)$, $V(P, s)$ and $V(s)$ are illustrated in Figure 1(b). Due to the page limit, the proof of Theorem 3 is provided in Appendix A.

Theorem 3 is the core idea for our algorithm design in Section 4. It indicates that the coupling solutions P_{ij} to the OT problem are always the same as its ROT version, and vice versa. In other words,

Corollary 1 (Translation-invariance of both the ROT solution and RW_2). *The coupling solutions to the quadratic ROT problem are invariant to any translation of distributions.*

Corollary 1 not only guarantees the robustness of RW_2 against translational shifts but also suggests that the coupling solution of a ROT problem (including the classical OT problem) can be calculated by finding a more “proper” cost matrix of a translated probability distribution pair. This helps us improve the numerical stability and reduce the time complexity in many practical conditions. We provide a detailed analysis in Section 4 and demonstrate it in Section 5.

Corollary 2 (Relationship between RW_2 and W_2). *Let s be the minimizer $\bar{\nu} - \bar{\mu}$, it follows that,*

$$W_2^2(\mu, \nu) = \|\bar{\mu} - \bar{\nu}\|_2^2 + RW_2^2(\mu, \nu). \quad (7)$$

Corollary 2 indicates that there exists a Pythagorean relationship among three types of distances, W_2 , RW_2 , and L_2 , as illustrated in Figure 1(c).

Corollary 2 provides a refinement to understand a distribution shift (measured by W_2) in the perspective of bias and variance decomposition. The L_2 Euclidean distance between the expectations of two distributions corresponds to the “bias” between two distributions, and the value of RW_2 corresponds to the difference of “variances” or the “shapes” of two distributions. When the source distribution is a Dirac distribution, the situation degenerates to a classical bias-variance decomposition.

4 RW_2 Sinkhorn Algorithm

Based on the first two properties of RW_2 , we design a variant of the Sinkhorn algorithm, named RW_2 Sinkhorn, to compute RW_2 under translational shift. Furthermore, we show the new algorithm can be used as a technique to compute W_2 distance, and it provides enhanced numerical stability and a reduction of time complexity when the difference between the means of two distributions is large.

4.1 RW_2 Algorithm Design

Based on Theorem 3 and Corollary 1, we propose the RW_2 Sinkhorn algorithm for computing RW_2 distance and coupling solution P_{ij} , which is described in Algorithm 1. The key idea of this algorithm involves precomputing the difference between the means of two distributions, as shown in Line 3. Subsequently, it addresses a specific instance of the optimal transport problem where the means of the two distributions are identical by a regular Sinkhorn algorithm. It is important to note that alternative algorithms, such as the network-simplex algorithm or the auction algorithm [Peyré and Cuturi, 2020], can also be employed to complete the specific instance procedure.

4.2 RW_2 Technique for W_2 Computation

With the observation of Corollary 2, we can also propose a new approach to compute the W_2 distance from the right side of the Equation (7).

When $\|\bar{\nu} - \bar{\mu}\|_2$ is large enough, this new RW_2 based technique has advantages than the regular Sinkhorn in terms of numerical stability and time complexity. We provide an analysis of this new approach in the rest of this section. In addition, experiment in Section 5.1 validates the analysis of our proposed RW_2 Sinkhorn algorithm for computing W_2 distance.

4.3 Numerical Stability

The division by zero is a known numerical issue of the Sinkhorn algorithm, as shown in Equation (4), and infinitesimal value often occurs in the exponential process of the (negative) cost matrix, that is, $K \leftarrow e^{-\frac{c}{\lambda}}$. The results of the Corollary 1 suggest that it is possible to switch to another “mutually translated” cost matrix under a relative translation s to increase the numerical stability while preserving the same coupling solutions.

Algorithm 1 RW_2 Sinkhorn Algorithm

- 1: **Input:** $\{x_i\}_{i=1}^{m_1}$, $\{y_j\}_{j=1}^{m_2}$, $\{a_i\}_{i=1}^{m_1}$, $\{b_j\}_{j=1}^{m_2}$, λ , ϵ .
 - 2: **Output:** RW_2 , P .
 - 3: $s \leftarrow \sum_{j=1}^{m_2} y_j b_j - \sum_{i=1}^{m_1} x_i a_i$
 - 4: **for** $i = 1$ **to** m_1 **do**
 - 5: **for** $j = 1$ **to** m_2 **do**
 - 6: $C_{ij} \leftarrow \|x_i + s - y_j\|_2^2$
 - 7: $K \leftarrow \exp(-C/\lambda)$
 - 8: $u^{(0)} \leftarrow e_{m_1}$, $v^{(0)} \leftarrow e_{m_2}$, $k \leftarrow 0$
 - 9: **repeat**
 - 10: $u^{(k+1)} \leftarrow a./ (K v^{(k)})$
 - 11: $v^{(k+1)} \leftarrow b./ (K^\top u^{(k+1)})$
 - 12: $P \leftarrow \text{diag}(u^{(k+1)}) K \text{diag}(v^{(k+1)})$
 - 13: $k \leftarrow k + 1$
 - 14: **until** $\|P e_{m_1} - a\|_2^2 + \|P^\top e_{m_2} - b\|_2^2 \leq \epsilon$
 - 15: $RW_2 \leftarrow \sum_{i=1}^{m_1} \sum_{j=1}^{m_2} P_{ij} C_{ij}$
 - 16: **return:** RW_2 , P
-

To measure the numerical stability of the matrix, we introduce $g(K)$, defined by the product of all entries K_{ij} . Since all entries K_{ij} are in the exponential format and lie in the range of $(0, 1]$, $g(K)$ is also in the range of $(0, 1]$. As $g(K)$ increases, most entries K_{ij} deviate from zero, which means numerical computation will be more stable. Because of the following transformation,

$$g(K) = \prod_{i=1}^{m_1} \prod_{j=1}^{m_2} K_{ij} = \prod_{i=1}^{m_1} \prod_{j=1}^{m_2} \exp\left(-\frac{C_{ij}}{\lambda}\right) = \exp\left(-\frac{\sum_{i=1}^{m_1} \sum_{j=1}^{m_2} \|x_i + s - y_j\|_2^2}{\lambda}\right),$$

one can choose the relative translation $s = \bar{y} - \bar{x}$, so that $g(K)$ can achieve its maximum. When we assume the probability mass on each data is equal, $\bar{y} - \bar{x}$ is the same as $\bar{\nu} - \bar{\mu}$.

4.4 Complexity Analysis

Altschuler et al. [2017] provided a proof for the time complexity of the optimal transport model by Sinkhorn algorithm with τ approximation, which is $O(m^2 \|C\|_\infty^3 (\log m) \tau^{-3})$, where $\|C\|_\infty = \max_{ij} C_{ij}$, with assuming $m = m_1 = m_2$ for the sake of simplicity. When the translated cost matrix has a smaller infinity norm $\|C\|_\infty$, we can see that the time complexity will be reduced. When two distributions are sub-Gaussian and $\|\bar{\nu} - \bar{\mu}\|_2$ is large enough, we can have a more rigorous analysis for the complexity analysis, which is provided in Appendix C. Our results from the first experiment in Section 5 also empirically validate this idea.

5 Experiments

To comprehensively evaluate and validate our proposed method, we conducted three experiments: numerical validation, digit recognition, and similar weather pattern detection. The three experiments are motivated differently: the first experiment is used to validate the numerical stability and computational time of the RW_2 Sinkhorn algorithm; the second experiment serves as validation of the robustness of RW_2 distance to the distribution translation in a real-world application; and the third experiment is to show the RW_2 can scale up to large-scale datasets to identify the similar weather patterns. All tests are executed on a workstation with a 2.60 GHz Intel Core i7 processor and 16GB of RAM using a single computation thread.

5.1 Numerical Validation

First we demonstrate the benefits of applying the RW_2 Sinkhorn algorithm for computing W_2 distance on specially designed examples. Let us consider two sets of data points randomly sampled from two identical distributions μ and ν , each with 1,000 samples. To compare the performance of Algorithm 1 and the classical Sinkhorn, we translate the distribution μ with a vector s , where the length of translation s ranges within $[0, 3]$. The idea is illustrated in Figure 2.

Experimental setting We compare the two versions of Sinkhorn algorithms in W_2 error and running time. We repeat each experiment and data sampling 10 times. We test a pair of Gaussian distributions in \mathbb{R} (Figure 3(a) and 3(d)), a pair of Gaussians in \mathbb{R}^{10} (Figure 3(b) and 3(e)), and a pair of uniform distributions in \mathbb{R}^{10} (Figure 3(c) and 3(e)). We set $\lambda = 0.1$ and $\epsilon = 0.01$ for both algorithms.

Experiment results Figure 3 shows that when the length of the translation increases, the proposed RW_2 Sinkhorn algorithm significantly outperforms the regular Sinkhorn algorithm in both the running time and computational errors. We also test the performance of the RW_2 Sinkhorn algorithm on other distributions. See more results in Appendix B.

5.2 Digit Recognition

We test the robustness of the RW_2 distance on the MNIST dataset, perturbed by random translations. Each digital image is a 28 x 28 grid and can be converted into a discrete probability distribution by normalizing the intensity on each pixel by the sum of all intensities. We consider a subset of N data points randomly sampled from the MNIST dataset, where $N = \{100, 1000\}$. We embed each image in a larger 84 x 84 grid and translate each image with a random vector s (varying lengths and directions). We test performance on the length of s ranging within $\{0, 4, 8, 12, 16, 20, 24, 28\}$ pixels.

Experimental setting We report the mean and standard deviation of classification error using a 1/4 test ratio scheme, repeated 10 times. We use the nearest neighbor search as a classifier with

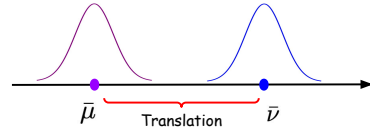


Figure 2: Schematic illustration of the first experiment. Assume that the distributions μ and ν are the same type of distribution. We compare the performance of Algorithm 1 and the classical Sinkhorn by translating the distribution μ along vector s , i.e., $s = \bar{\nu} - \bar{\mu}$.

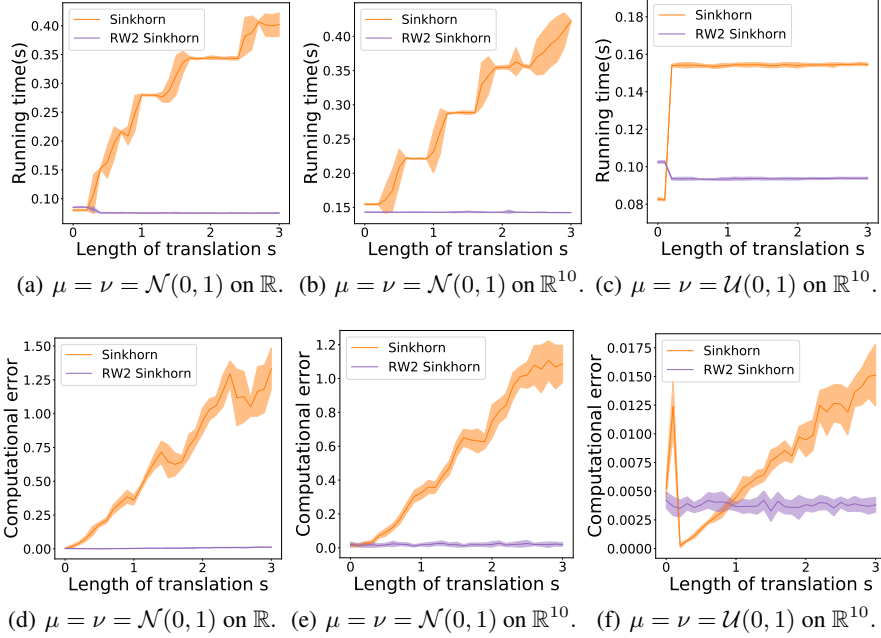


Figure 3: Comparison of the RW_2 Sinkhorn algorithm and the classic Sinkhorn in running time and computational error. When the translation is small, the Sinkhorn algorithm with RW_2 technique performs similarly or slightly worse than the classical Sinkhorn algorithm. As the translation grows, the Sinkhorn algorithm with RW_2 technique significantly outperforms the regular Sinkhorn algorithm.

RW_2 distance, as well as other distances (L_1, L_2, W_1, W_2) as the baselines. We set the $\lambda = 0.1$ and $\epsilon = 0.1$ for the RW_2 Sinkhorn algorithm.

Experiment results Figure 4 shows that RW_2 distance significantly outperforms the other distances when the translation s is large in both sample sizes $N = 100$ and $N = 1,000$.

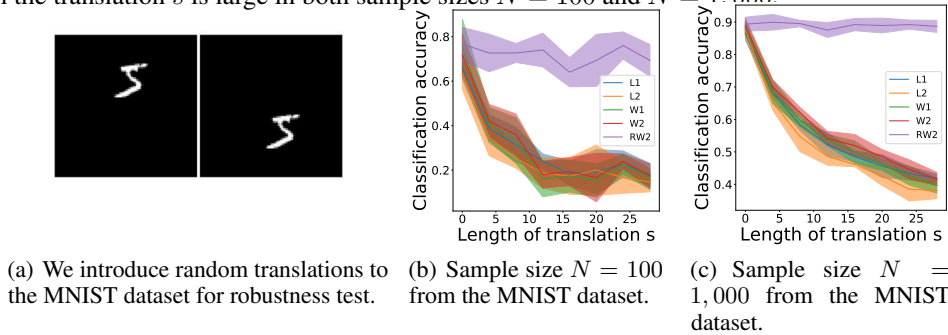


Figure 4: Classification accuracy performance of the nearest neighbor search with RW_2 distance and other baseline distances (L_1, L_2, W_1, W_2) on MNIST dataset. Subfigure (a) shows both the train and test images are perturbed by random translations. Subfigures (b) and (c) show that the RW_2 distance is more robust than the other distances against the translational shift.

5.3 Similar Thunderstorm Pattern Detection

We apply RW_2 distance on the real-world thunderstorm dataset, to show that RW_2 can be used for identifying similar weather patterns and focus more on shape similarity compared with W_2 distance. Our data are radar images from MULTI-RADAR/MULTI-SENSOR SYSTEM (MRMS) [Zhang et al., 2016] with a $150 \text{ km} \times 150 \text{ km}$ rectangular area centered at the Dallas Fort Worth International Airport (DFW), where each pixel represents a $3 \text{ km} \times 3 \text{ km}$ area. The data is assimilated every 10 minutes tracking a long time range of history from 2014 to 2022, with 205,848 images in total. Vertically Integrated Liquid Density (VIL density) and reflectivity are two common measurements for assessing thunderstorm intensity, with threshold values of $3 \text{ kg} \cdot \text{m}^{-3}$ and 35 dBZ , respectively

[Matthews and Delaura, 2010]. For the sake of simplicity, we will focus on reflectivity as our main indicator for thunderstorm intensity.

We consider two types of thunderstorm events: thunderstorm snapshots and thunderstorm sequences. More comparison results can be found in the Appendix B.

Experimental setting We apply the RW_2 Sinkhorn algorithm to compute both the W_2 distance and the RW_2 distance to identify the most similar thunderstorm event given a reference event, with $\lambda = 0.1$ and $\epsilon = 0.01$. For the thunderstorm sequence identification, we consider a one-hour thunderstorm event as our reference, consisting of 6 images in time order.

Thunderstorm snapshot results Given the same reference thunderstorm snapshot, Figure 5 shows that the similar events identified by RW_2 focus more on shape similarity compared with W_2 .

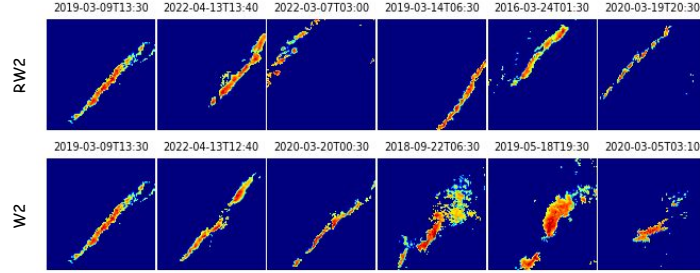


Figure 5: Thunderstorm snapshot comparison using RW_2 and W_2 . The leftmost images in the first column are the same reference thunderstorm event. The other images show the top 5 most similar thunderstorm snapshots identified by RW_2 and W_2 , sorted in order of similarity. The RW_2 distance focuses more on shape similarity, while the W_2 distance pays more attention to location similarity. As observed, the last three images from W_2 show much less pattern similarity with the reference.

Thunderstorm sequence results Given a reference thunderstorm sequence, Figure 6 shows that the similar sequences identified by RW_2 focus more on shape similarity compared with W_2 .

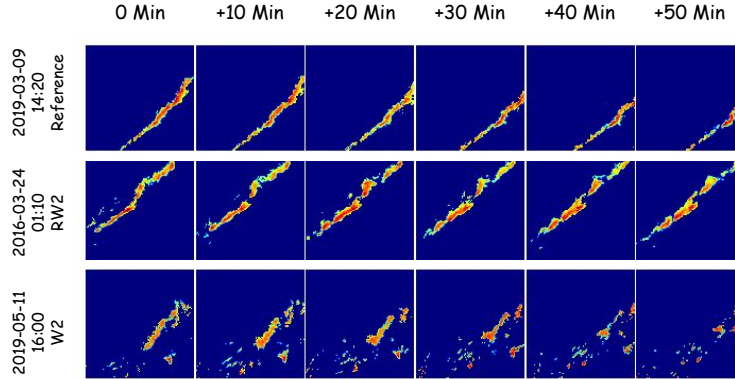


Figure 6: Similar thunderstorm sequence identification using RW_2 and W_2 . The first row is the reference thunderstorm sequence with 1-hour duration. The second and third rows are the most similar thunderstorm sequences identified by RW_2 and W_2 . Again we observe that RW_2 focuses more on pattern (shape) similarity, and W_2 gets distracted by location similarity.

6 Conclusions

In this paper, we introduce a new family of distances, relative-translation invariant Wasserstein (RW_p) distances, for measuring the pattern similarity between two probability distributions (and their data supports). Generalizing from the classical optimal transport model, we show that the proposed RW_p distances are real distance metrics defined on the quotient set $\mathcal{P}_p(\mathbb{R}^n)/\sim$ and invariant to the translations of distributions. When $p = 2$, this distance enjoys more useful properties, including decomposability of the reformulated optimal transport model, translation-invariance of coupling solutions and RW_2 , and Pythagorean relationship of RW_2 and W_2 distances. Based on these properties, we show a distribution shift, measured by W_2 distance, which can be explained from the perspective of bias-variance. In addition, we propose a variant of the Sinkhorn algorithm, named RW_2 Sinkhorn algorithm, for efficiently calculating RW_2 distance, coupling solutions, as

well as W_2 distance. We provide the analysis of numerical stability and time complexity for the proposed algorithm. Finally, we validate the RW_2 distance metric and the algorithm performance with illustrative and real-world experiments. The experimental results report that our proposed algorithm significantly improves the computational efficiency of Sinkhorn in practical applications with large translations, and the RW_2 distance is robust to distribution translations compared with baselines.

References

- Optimal Transport: Theory and Applications*. London Mathematical Society Lecture Note Series. Cambridge University Press, 2014.
- Jason Altschuler, Jonathan Niles-Weed, and Philippe Rigollet. Near-linear time approximation algorithms for optimal transport via Sinkhorn iteration. In *Advances in Neural Information Processing Systems*, volume 30, 2017.
- David Alvarez-Melis, Stefanie Jegelka, and Tommi S. Jaakkola. Towards optimal transport with global invariances. In Kamalika Chaudhuri and Masashi Sugiyama, editors, *Proceedings of the Twenty-Second International Conference on Artificial Intelligence and Statistics*, volume 89 of *Proceedings of Machine Learning Research*, pages 1870–1879. PMLR, 16–18 Apr 2019.
- Luigi Ambrosio, Nicola Gigli, and Giuseppe Savare. Gradient flows in metric spaces and in the space of probability measures. *Lectures in Mathematics, ETH Zurich*, January 2005.
- Martin Arjovsky, Soumith Chintala, and Léon Bottou. Wasserstein generative adversarial networks. In *Proceedings of the 34th International Conference on Machine Learning*, volume 70 of *Proceedings of Machine Learning Research*, pages 214–223. PMLR, 06–11 Aug 2017.
- Ruidi Chen and Ioannis Ch Paschalidis. A robust learning approach for regression models based on distributionally robust optimization. *Journal of Machine Learning Research*, 19(13):1–48, 2018.
- Samantha Chen and Yusu Wang. Neural approximation of wasserstein distance via a universal architecture for symmetric and factorwise group invariant functions. In *Advances in Neural Information Processing Systems*, volume 36, pages 9506–9517, 2023.
- Lenaic Chizat. *Unbalanced Optimal Transport : Models, Numerical Methods, Applications*. PhD thesis, 11 2017.
- Julien Grand Clement and Christian Kroer. First-Order Methods for Wasserstein Distributionally Robust MDP. In *Proceedings of the 38th International Conference on Machine Learning*, volume 139 of *Proceedings of Machine Learning Research*, pages 2010–2019, 18–24 Jul 2021.
- Roberto Cominetti and Jaime San Martín. Asymptotic analysis of the exponential penalty trajectory in linear programming. *Mathematical Programming*, 67:169–187, 1994.
- Nicolas Courty, Rémi Flamary, Amaury Habrard, and Alain Rakotomamonjy. Joint distribution optimal transportation for domain adaptation. *Advances in Neural Information Processing Systems*, 30, 2017a.
- Nicolas Courty, Rémi Flamary, Devis Tuia, and Alain Rakotomamonjy. Optimal transport for domain adaptation. *IEEE Transactions on Pattern Analysis and Machine Intelligence*, 39(9):1853–1865, 2017b.
- Marco Cuturi. Sinkhorn distances: Lightspeed computation of optimal transport. *Advances in neural information processing systems*, 26, 2013.
- Bharath Bhushan Damodaran, Benjamin Kellenberger, Rémi Flamary, Devis Tuia, and Nicolas Courty. DeepJDOT: Deep joint distribution optimal transport for unsupervised domain adaptation. In *Proceedings of the European conference on computer vision (ECCV)*, pages 447–463, 2018.
- Michael Dixon and Gerry Wiener. Titan: Thunderstorm identification, tracking, analysis, and nowcasting—a radar-based methodology. *Journal of Atmospheric and Oceanic Technology*, 10(6): 785 – 797, 1993.

- Jiaojiao Fan, Qinsheng Zhang, Amirhossein Taghvaei, and Yongxin Chen. Variational Wasserstein gradient flow. In *Proceedings of the 39th International Conference on Machine Learning*, volume 162 of *Proceedings of Machine Learning Research*, pages 6185–6215, 17–23 Jul 2022.
- Wenshuo Guo, Nhat Ho, and Michael Jordan. Fast algorithms for computational optimal transport and Wasserstein barycenter. In *Proceedings of the Twenty Third International Conference on Artificial Intelligence and Statistics*, volume 108 of *Proceedings of Machine Learning Research*, pages 2088–2097, 26–28 Aug 2020.
- Martin Heusel, Hubert Ramsauer, Thomas Unterthiner, Bernhard Nessler, and Sepp Hochreiter. GANs trained by a two time-scale update rule converge to a local nash equilibrium. In *Proceedings of the 31st International Conference on Neural Information Processing Systems*, page 6629–6640, 2017.
- Hicham Janati, Marco Cuturi, and Alexandre Gramfort. Spatio-temporal alignments: Optimal transport through space and time. In *Proceedings of the Twenty Third International Conference on Artificial Intelligence and Statistics*, volume 108 of *Proceedings of Machine Learning Research*, pages 1695–1704, 26–28 Aug 2020.
- Alexander Korotin, Lingxiao Li, Justin Solomon, and Evgeny Burnaev. Continuous Wasserstein-2 barycenter estimation without minimax optimization, 2021.
- Alexander Korotin, Vage Egiazarian, Lingxiao Li, and Evgeny Burnaev. Wasserstein iterative networks for barycenter estimation. In *Advances in Neural Information Processing Systems*, volume 35, pages 15672–15686. Curran Associates, Inc., 2022.
- Khang Le, Dung Q Le, Huy Nguyen, Dat Do, Tung Pham, and Nhat Ho. Entropic gromov-Wasserstein between Gaussian distributions. In *Proceedings of the 39th International Conference on Machine Learning*, volume 162 of *Proceedings of Machine Learning Research*, pages 12164–12203, 17–23 Jul 2022.
- Tianyi Lin, Nhat Ho, Xi Chen, Marco Cuturi, and Michael Jordan. Fixed-support Wasserstein barycenters: Computational hardness and fast algorithm. In *Advances in Neural Information Processing Systems*, volume 33, pages 5368–5380, 2020.
- Guillaume Mahey, Laetitia Chapel, Gilles Gasso, Clément Bonet, and Nicolas Courty. Fast optimal transport through sliced generalized Wasserstein geodesics. In *Advances in Neural Information Processing Systems*, volume 36, pages 35350–35385, 2023.
- Michael Matthews and Rich Delaura. Assessment and Interpretation of En Route Weather Avoidance Fields from the Convective Weather Avoidance Model. In *10th AIAA Aviation Technology, Integration, and Operations (ATIO) Conference*, September 2010.
- Petr Mokrov, Alexander Korotin, Lingxiao Li, Aude Genevay, Justin M Solomon, and Evgeny Burnaev. Large-scale Wasserstein gradient flows. In *Advances in Neural Information Processing Systems*, volume 34, pages 15243–15256, 2021.
- Khai Nguyen and Nhat Ho. Revisiting sliced Wasserstein on images: From vectorization to convolution. In *Advances in Neural Information Processing Systems*, volume 35, pages 17788–17801, 2022.
- Khai Nguyen and Nhat Ho. Energy-based sliced Wasserstein distance. In *Advances in Neural Information Processing Systems*, volume 36, pages 18046–18075, 2023.
- Quang Minh Nguyen, Hoang H. Nguyen, Yi Zhou, and Lam M. Nguyen. On unbalanced optimal transport: gradient methods, sparsity and approximation error. *J. Mach. Learn. Res.*, 24(1), Mar 2024.
- Gabriel Peyré and Marco Cuturi. Computational optimal transport, 2020.
- Pedro H. O. Pinheiro. Unsupervised domain adaptation with similarity learning. *2018 IEEE/CVF Conference on Computer Vision and Pattern Recognition*, pages 8004–8013, 2017.

- Nigel M. Roberts and Humphrey W. Lean. Scale-selective verification of rainfall accumulations from high-resolution forecasts of convective events. *Monthly Weather Review*, 136(1):78 – 97, 2008.
- Paul-Edouard Sarlin, Daniel DeTone, Tomasz Malisiewicz, and Andrew Rabinovich. SuperGlue: Learning Feature Matching With Graph Neural Networks. *2020 IEEE/CVF Conference on Computer Vision and Pattern Recognition (CVPR)*, pages 4937–4946, 2019.
- Thibault Sejourne, Francois-Xavier Vialard, and Gabriel Peyré. The Unbalanced Gromov Wasserstein Distance: Conic Formulation and Relaxation. In *Advances in Neural Information Processing Systems*, volume 34, pages 8766–8779, 2021.
- Soroosh Shafieezadeh-Abadeh, Peyman Mohajerin Esfahani, and Daniel Kuhn. Distributionally robust logistic regression. In *Neural Information Processing Systems*, 2015.
- Jian Shen, Yanru Qu, Weinan Zhang, and Yong Yu. Wasserstein distance guided representation learning for domain adaptation. In *AAAI Conference on Artificial Intelligence*, 2017.
- Ilya O. Tolstikhin, Olivier Bousquet, Sylvain Gelly, and Bernhard Schölkopf. Wasserstein auto-encoders. *ArXiv*, abs/1711.01558, 2017.
- Tomas Vaskevicius and Lénaïc Chizat. Computational Guarantees for Doubly Entropic Wasserstein Barycenters. In *Advances in Neural Information Processing Systems*, volume 36, pages 12363–12388. Curran Associates, Inc., 2023.
- Roman Vershynin. *High-dimensional probability: An introduction with applications in data science*, volume 47. Cambridge university press, 2018.
- C. Villani and American Mathematical Society. *Topics in Optimal Transportation*. Graduate studies in mathematics. American Mathematical Society, 2003.
- Cédric Villani. *Optimal transport: Old and new*. Springer, Berlin, Heidelberg., 2009.
- Binshuai Wang, James Pinto, and Peng Wei. *Identifying Similar Thunderstorm Sequences for Airline Decision Support via Optimal Transport Theory*. 2023.
- Zhuodong Yu, Ling Dai, Shaohang Xu, Siyang Gao, and Chin Pang Ho. Fast Bellman Updates for Wasserstein Distributionally Robust MDPs. In A. Oh, T. Naumann, A. Globerson, K. Saenko, M. Hardt, and S. Levine, editors, *Advances in Neural Information Processing Systems*, volume 36, pages 30554–30578. Curran Associates, Inc., 2023.
- Jian Zhang, Kenneth Howard, Carrie Langston, Brian Kaney, Youcun Qi, Lin Tang, Heather Grams, Yadong Wang, Stephen Cocks, Steven Martinaitis, Ami Arthur, Karen Cooper, Jeff Brogden, and David Kitzmiller. Multi-Radar Multi-Sensor (MRMS) Quantitative Precipitation Estimation: Initial Operating Capabilities. *Bulletin of the American Meteorological Society*, 97(4):621 – 638, 2016.

A Main Proofs

A.1 Theorem 1

Proof of Theorem 1. It is clear to verify that when $\|s\|_p \geq 2 \max_{i,j} \|x_i - y_j\|_p$, for any $i, j, (1 \leq i \leq m_1, 1 \leq j \leq m_2)$, it follows that $\|x_i + s - y_j\|_p \geq \|s\|_p - \|x_i - y_j\|_p \geq 2 \max_{i,j} \|x_i - y_j\|_p - \|x_i - y_j\|_p \geq \|x_i - y_j\|_p$. In other words, when $\|s\|_p \geq 2 \max_{i,j} \|x_i - y_j\|_p$, the relative distance between each pair of support x_i and y_j are always greater than or equal to the non-translated distance, which implies the total transport cost for the translated case will also greater than or equal to the cost for the non-translated distance. Since we are trying to find the minimal value, we can only focus on the compact set $\{s \in \mathbb{R}^n \mid \|s\|_p \leq 2 \max_{i,j} \|x_i - y_j\|_p\}$. \square

A.2 Theorem 2

Proof of Theorem 2. With the previous notations, firstly, we will show that the translation relation \sim is an equivalence relation on set $\mathcal{P}_p(\mathbb{R}^n)$.

Equivalence relation requires reflexivity, symmetry, and transitivity, and the following observations show translation relation is indeed an equivalence relation.

- Reflexivity, $(x \sim x)$.

For any distribution $\mu \in \mathcal{P}_p(\mathbb{R}^n)$, it can translate to itself with zero vector.

- Symmetry, $(x \sim y \implies y \sim x)$.

For any distribution $\mu, \nu \in \mathcal{P}_p(\mathbb{R}^n)$, if μ can be translated to ν , then ν can also be translated to μ .

- Transitivity, $(x \sim y \text{ and } y \sim z \implies x \sim z)$.

For any distribution $\mu, \nu, \eta \in \mathcal{P}_p(\mathbb{R}^n)$, if μ can be translated to ν , and ν can be translated to η , then μ can also be translated to η .

Based on the property of equivalence relation, it is clear that set $\mathcal{P}_p(\mathbb{R}^n)/\sim$ is well-defined. Let $[\mu]$ be an element in set M/\sim , where μ is a representative of $[\mu]$, i.e. $[\mu]$ is the set of distributions that can be mutually translated from μ . Noticing that $W_p(\cdot, \cdot)$ is a real distance metric on $\mathcal{P}_p(\mathbb{R}^n)$ [Villani and Society, 2003], it implies that $W_p(\cdot, \cdot)$ satisfied with identity, positivity, symmetry, and the triangle inequality. Based on $W_p(\cdot, \cdot)$, we show $RW_p(\cdot, \cdot)$ satisfies with identity, positivity, symmetry, and triangle inequality with respect to elements in $\mathcal{P}_p(\mathbb{R}^n)/\sim$.

For any $\mu, \nu, \eta \in \mathcal{P}_p(\mathbb{R}^n)/\sim$,

- Identity,

$$RW_p([\mu], [\mu]) = \min_{\mu \in [\mu], \mu \in [\mu]} [W_p(\mu, \mu)] = 0.$$

- Positivity,

$$RW_p([\mu], [\nu]) = \min_{\mu \in [\mu], \nu \in [\nu]} [W_p(\mu, \nu)] \geq 0.$$

- Symmetry,

$$RW_p(\mu, \nu) = \min_{\mu \in [\mu], \nu \in [\nu]} [W_p(\mu, \nu)] = \min_{\nu \in [\nu], \mu \in [\mu]} [W_p(\nu, \mu)] = RW_p(\nu, \mu).$$

- Triangle inequality,

$$\begin{aligned}
& RW_p(\mu, \nu) \\
&= \min_{\mu \in [\mu], \nu \in [\nu]} [W_p(\mu, \nu)] \\
&\leq \min_{\eta, \eta' \in [\eta]} \min_{\mu \in [\mu], \nu \in [\nu]} [W_p(\mu, \eta) + W_p(\eta, \eta') + W_p(\eta', \nu)] \\
&= \min_{\mu \in [\mu], \nu \in [\nu], \eta, \eta' \in [\eta]} [W_p(\mu, \eta) + 0 + W_p(\eta', \nu)] \\
&= \min_{\mu \in [\mu], \eta \in [\eta]} [W_p(\mu, \eta)] + \min_{\nu \in [\nu], \eta' \in [\eta]} [W_p(\eta', \nu)] \\
&= \min_{\mu \in [\mu], \eta \in [\eta]} [W_p(\mu, \eta)] + \min_{\nu \in [\nu], \eta \in [\eta]} [W_p(\eta, \nu)] \\
&= RW_p(\mu, \eta) + RW_p(\eta, \nu).
\end{aligned}$$

□

A.3 Theorem 3

Proof of Theorem 3. With the previous notations, firstly, we show the two-stage optimization problem, $\min_{s \in \mathbb{R}^n} \min_{P \in \Pi(\mu, \nu)} H(P, s)$, can be decomposed into two independent one-stage optimization problems,

$$\min_{P \in \Pi(\mu, \nu)} (E(P)) \text{ and } \min_{s \in \mathbb{R}^n} (V(s)).$$

For the objective function $H(P, s)$, we expand it with respect to s ,

$$\begin{aligned}
& H(P, s) \\
&= \sum_{i=1}^{m_1} \sum_{j=1}^{m_2} \|x_i + s - y_j\|_2^2 P_{ij} \\
&= \sum_{i=1}^{m_1} \sum_{j=1}^{m_2} \left(\|x_i - y_j\|_2^2 + \|s\|_2^2 + 2s \cdot (x_i - y_j) \right) P_{ij} \tag{8} \\
&= \sum_{i=1}^{m_1} \sum_{j=1}^{m_2} \|x_i - y_j\|_2^2 P_{ij} + \sum_{i=1}^{m_1} \sum_{j=1}^{m_2} \|s\|_2^2 P_{ij} + 2 \sum_{i=1}^{m_1} \sum_{j=1}^{m_2} s \cdot (x_i - y_j) P_{ij}.
\end{aligned}$$

We can rewrite the second and the third terms in Equation (8) under the condition $P \in \Pi(\mu, \nu)$, which implies that,

$$\sum_{i=1}^{m_1} \sum_{j=1}^{m_2} P_{ij} = 1, \sum_{j=1}^{m_2} P_{ij} = a_i, \sum_{i=1}^{m_1} P_{ij} = b_j, 1 \leq i \leq m_1, 1 \leq j \leq m_2.$$

For the second term, it follows that

$$\sum_{i=1}^{m_1} \sum_{j=1}^{m_2} \|s\|_2^2 P_{ij} = \|s\|_2^2 \cdot \left(\sum_{i=1}^{m_1} \sum_{j=1}^{m_2} P_{ij} \right) = \|s\|_2^2 \cdot 1 = \|s\|_2^2.$$

For the third term, it follows that

$$\begin{aligned}
& 2 \sum_{i=1}^{m_1} \sum_{j=1}^{m_2} s \cdot (x_i - y_j) P_{ij} \\
&= 2s \cdot \sum_{i=1}^{m_1} \sum_{j=1}^{m_2} (x_i - y_j) P_{ij} \\
&= 2s \cdot \left(\sum_{i=1}^{m_1} \sum_{j=1}^{m_2} x_i \cdot P_{ij} - \sum_{i=1}^{m_1} \sum_{j=1}^{m_2} y_j \cdot P_{ij} \right) \\
&= 2s \cdot \left(\sum_{i=1}^{m_1} x_i \cdot \left(\sum_{j=1}^{m_2} P_{ij} \right) - \sum_{j=1}^{m_2} y_j \cdot \left(\sum_{i=1}^{m_1} P_{ij} \right) \right) \\
&= 2s \cdot \left(\sum_{i=1}^{m_1} x_i \cdot a_i - \sum_{j=1}^{m_2} y_j \cdot b_j \right) \\
&= 2s \cdot (\bar{\mu} - \bar{\nu}).
\end{aligned}$$

Thus, we have the following transformation,

$$\begin{aligned}
& \min_{s \in \mathbb{R}^n} \min_{P \in \Pi(\mu, \nu)} H(P, s) \\
&= \min_{s \in \mathbb{R}^n} \min_{P \in \Pi(\mu, \nu)} \left(\sum_{i=1}^{m_1} \sum_{j=1}^{m_2} \|x_i - y_j\|_2^2 P_{ij} + \sum_{i=1}^{m_1} \sum_{j=1}^{m_2} \|s\|_2^2 P_{ij} + 2 \sum_{i=1}^{m_1} \sum_{j=1}^{m_2} s \cdot (x_i - y_j) P_{ij} \right) \\
&= \min_{s \in \mathbb{R}^n} \min_{P \in \Pi(\mu, \nu)} \sum_{i=1}^{m_1} \sum_{j=1}^{m_2} \|x_i - y_j\|_2^2 P_{ij} + \min_{s \in \mathbb{R}^n} \min_{P \in \Pi(\mu, \nu)} \left(\sum_{i=1}^{m_1} \sum_{j=1}^{m_2} \|s\|_2^2 P_{ij} + 2 \sum_{i=1}^{m_1} \sum_{j=1}^{m_2} s \cdot (x_i - y_j) P_{ij} \right) \\
&= \min_{s \in \mathbb{R}^n} \min_{P \in \Pi(\mu, \nu)} \sum_{i=1}^{m_1} \sum_{j=1}^{m_2} \|x_i - y_j\|_2^2 P_{ij} + \min_{s \in \mathbb{R}^n} (\|s\|_2^2 + 2s \cdot (\bar{\mu} - \bar{\nu})) \\
&= \min_{P \in \Pi(\mu, \nu)} \sum_{i=1}^{m_1} \sum_{j=1}^{m_2} \|x_i - y_j\|_2^2 P_{ij} + \min_{s \in \mathbb{R}^n} (\|s\|_2^2 + 2s \cdot (\bar{\mu} - \bar{\nu})) \\
&= \min_{P \in \Pi(\mu, \nu)} (E(P)) + \min_{s \in \mathbb{R}^n} (V(s))
\end{aligned}$$

Since $V(s)$ is a high-dimensional quadratic function of variable s , it is easy to follow that the minimum is achieved when $s = \bar{\nu} - \bar{\mu}$.

□

B Additional Experiment Results

B.1 Additional experiment results for Section 5.1 - Numerical Validation

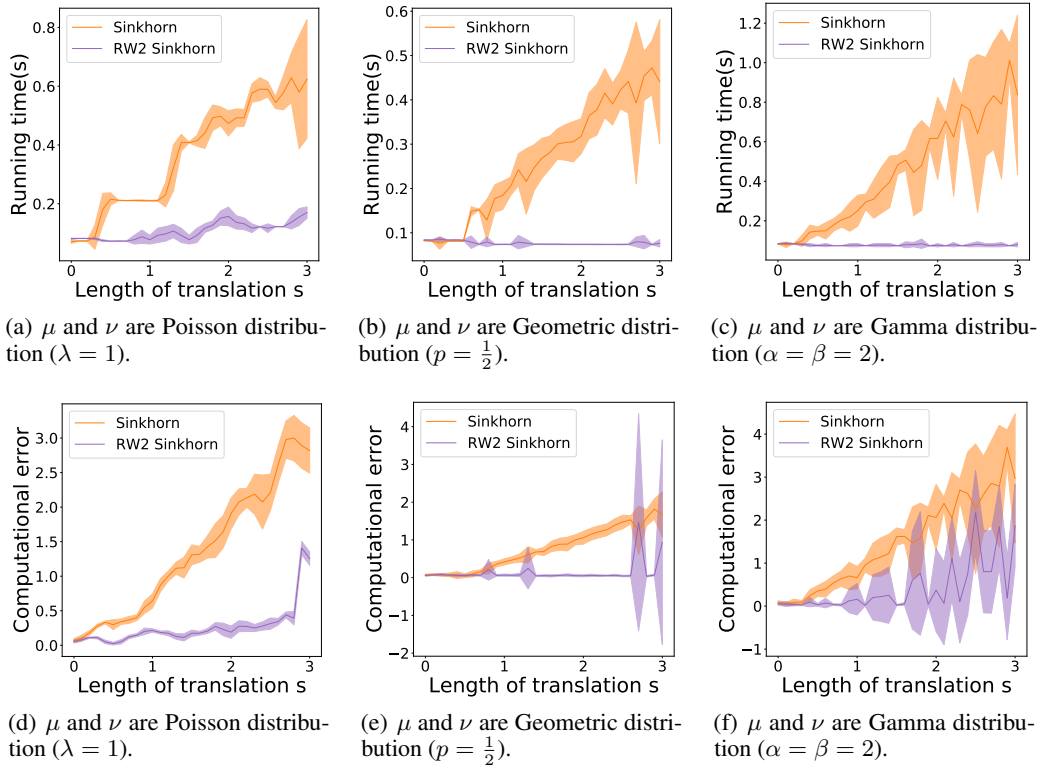


Figure 7: Additional results from the experiment in Section 5.1. The first column shows the results from a pair of Poisson distributions, the second column shows the results from a pair of Geometric distributions, and the third column shows the results from a pair of Gamma distributions, all of which are defined on \mathbb{R} .

B.2 Additional experiment results for Section 5.3 - Similar Thunderstorm Pattern Detection

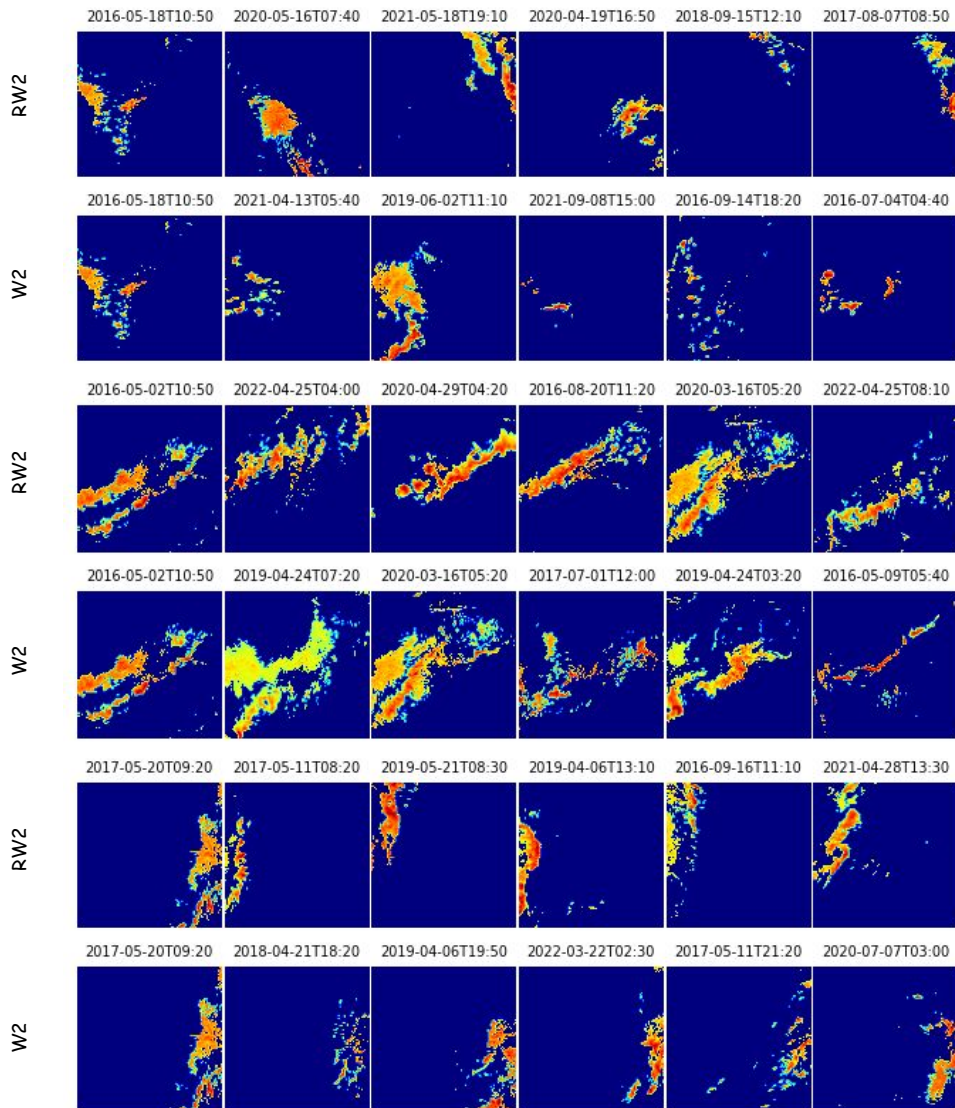


Figure 8: Three additional examples of similar thunderstorm snapshot identification using RW_2 and W_2 . The leftmost images in the first column are the reference thunderstorm events, which are 2016-05-18-10:50, 2016-05-02-10:50, and 2017-05-20-09:20. The other images show the top 5 most similar thunderstorm snapshots identified by RW_2 and W_2 , sorted in order of similarity.

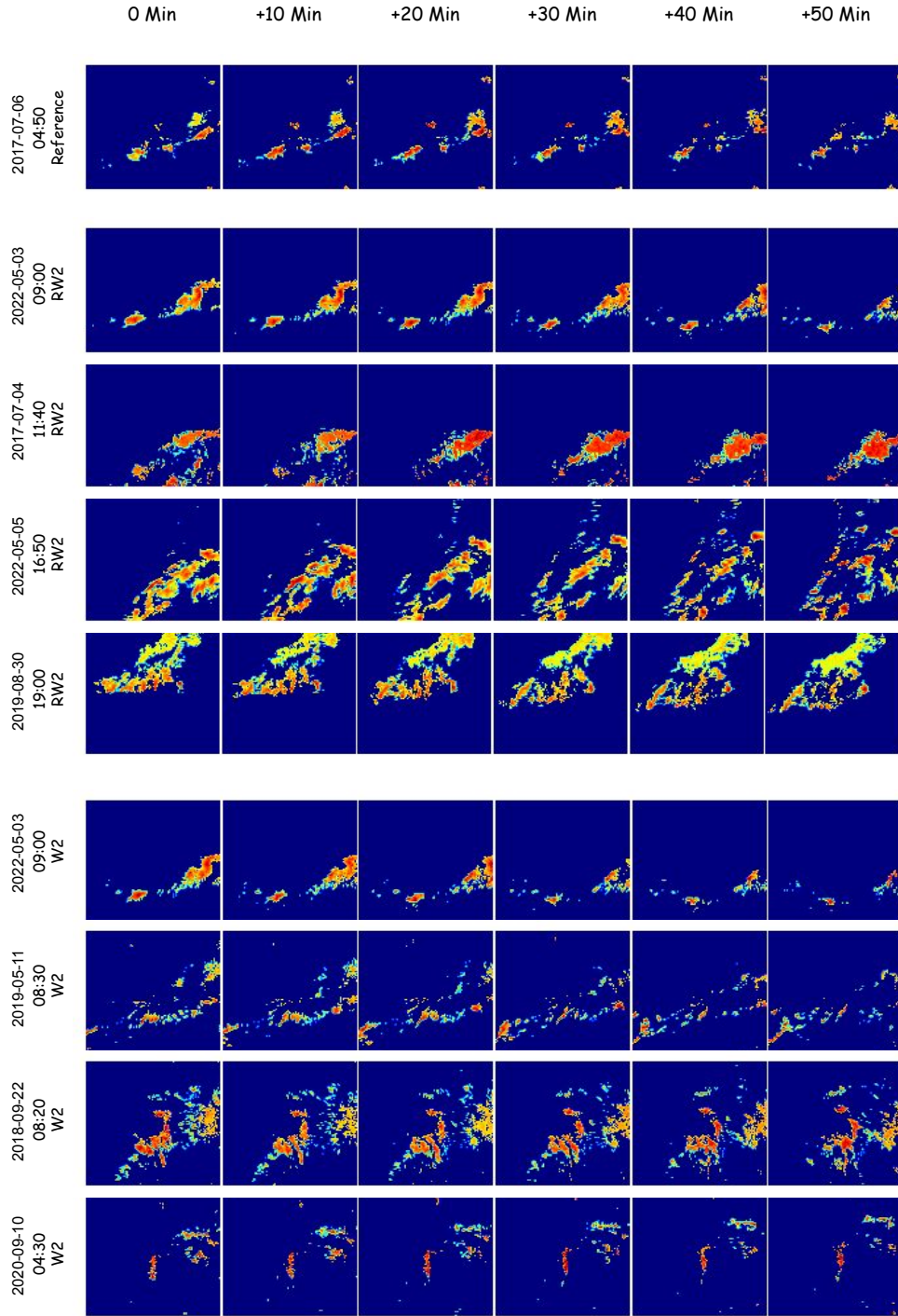


Figure 9: Similar thunderstorm sequence identification using RW_2 and W_2 . The first row is the reference thunderstorm sequence with a 1-hour duration. The second to the fifth rows are the top 4 most similar thunderstorm sequences identified by RW_2 . The sixth to the ninth rows are the top 4 most similar thunderstorm sequences identified by W_2 . Again we observe that RW_2 focuses more on pattern (shape) similarity, and W_2 gets distracted by location similarity.

C Complexity Analysis for Algorithm 1 under sub-Gaussian Distributions

This section is organized as follows. In section C.1, we state and prove the theorem regarding the time complexity of Algorithm 1. We leave the definitions and theorems used in the proof to section C.2.

C.1 Theoretical Results of Time Complexity

Assuming the two distributions are sub-Gaussian and $\|\bar{\nu} - \bar{\mu}\|_2^2$ is large enough, we can prove that with high probability, the translated cost matrix has a smaller norm $\|C\|_\infty$, thus the time complexity can be reduced.

Theorem 4. *Let μ, ν be two high-dimensional sub-Gaussian distributions in \mathbb{R}^n . $(X_1, X_2, \dots, X_{m_1}), (Y_1, Y_2, \dots, Y_{m_2})$ are i.i.d data sampled from μ and ν separately. Let $\bar{\mu} = \mathbb{E}\mu, \bar{\nu} = \mathbb{E}\nu, \bar{X} = \sum_{i=1}^{m_1} X_i/m_1, \bar{Y} = \sum_{i=1}^{m_2} Y_i/m_2$. Assume $\|\mu - \bar{\mu}\|_{\psi_2} < \infty, \|\nu - \bar{\nu}\|_{\psi_2} < \infty. l = \|\bar{\mu} - \bar{\nu}\|_2$. If*

$$l \geq C\sqrt{n} \left[1 + \|\mu - \bar{\mu}\|_{\psi_2} + \|\nu - \bar{\nu}\|_{\psi_2} \right] + C \left[\sqrt{\log(4m_1/\delta)} \cdot \|\mu - \bar{\mu}\|_{\psi_2} + \sqrt{\log(4m_2/\delta)} \cdot \|\nu - \bar{\nu}\|_{\psi_2} \right],$$

where C is an absolute constant, then with probability at least $1 - \delta$, we have

$$\max_{i,j} \|X_i - \bar{X} - Y_j + \bar{Y}\|_2 \leq \max_{i,j} \|X_i - Y_j\|_2.$$

Remark 1. *Sub-Gaussian distributions represent a broad class of distributions that encompass many common types, including multivariate normal distribution, multivariate symmetric Bernoulli, and uniform distribution on the sphere. Theorem ?? demonstrates that when the translation is significant, the maximum absolute entry of the cost matrix $\|C\|_\infty = \max_{i,j} |C_{ij}|$ tends to decrease. Consequently, our RW_2 method achieves better time complexity compared to W_2 . This theoretical finding is consistent with our experimental results, as shown in Figure 3.*

Proof of Theorem 4. For $i = 1, 2, \dots, m_1$, $X_i - \bar{\mu}$ is a sub-Gaussian random vector. Using Theorem 6 and taking a union bound over all the random vectors, we have for all X_i with probability at least $1 - \delta/4$, the following inequality holds

$$\|X_i - \bar{\mu}\|_2 \leq c(\sqrt{n} + \sqrt{\log(4m_1/\delta)}) \cdot \|\mu - \bar{\mu}\|_{\psi_2}. \quad (9)$$

Similarly, we have for all Y_j , with probability at least $1 - \delta$, the following inequality holds

$$\|Y_j - \bar{\nu}\|_2 \leq c(\sqrt{n} + \sqrt{\log(4m_2/\delta)}) \cdot \|\nu - \bar{\nu}\|_{\psi_2}. \quad (10)$$

Using Theorem 5, $\sum_{i=1}^{m_1} (X_i - \bar{\mu})$ is a sub-Gaussian random vector, with $\|\sum_{i=1}^{m_1} (X_i - \bar{\mu})\|_{\psi_2} \leq \sqrt{C \sum_{i=1}^{m_1} \|X_i - \bar{\mu}\|_{\psi_2}^2}$. Then using Theorem 6, with probability at least $1 - \delta/4$, we have

$$\begin{aligned} \left\| \sum_{i=1}^{m_1} X_i - m_1 \bar{\mu} \right\|_2 &\leq c(\sqrt{n} + \sqrt{\log(1/\delta)}) \cdot \left\| \sum_{i=1}^{m_1} (X_i - \bar{\mu}) \right\|_{\psi_2} \\ &= c(\sqrt{n} + \sqrt{\log(1/\delta)}) \cdot \sqrt{C \sum_{i=1}^{m_1} \|X_i - \bar{\mu}\|_{\psi_2}^2} \\ &= c'(\sqrt{n} + \sqrt{\log(1/\delta)}) \cdot \sqrt{m_1} \|\mu - \bar{\mu}\|_{\psi_2}, \end{aligned} \quad (11)$$

where c' is an absolute constant. Similarly, with probability at least $1 - \delta$, we have

$$\left\| \sum_{j=1}^{m_2} Y_j - m_2 \bar{\nu} \right\|_2 \leq c'(\sqrt{n} + \sqrt{\log(1/\delta)}) \cdot \sqrt{m_2} \|\nu - \bar{\nu}\|_{\psi_2}, \quad (12)$$

where c' is an absolute constant. In the following proof, we consider the union bound of all the high-probability events above, such that (9), (10), (11) and (12) hold. It occurs with probability at

least $1 - \delta$.

First, for $\max_{i,j} \|X_i - Y_j\|_2$, we have

$$\begin{aligned} \max_{i,j} \|X_i - Y_j\|_2 &\geq \max_{i,j} \|\bar{\mu} - \bar{\nu}\|_2 - \|X_i - \bar{\mu}\|_2 - \|Y_j - \bar{\nu}\|_2 \\ &\geq l - \left[c(\sqrt{n} + \sqrt{\log(4m_1/\delta)}) \cdot \|\mu - \bar{\mu}\|_{\psi_2} \right] \\ &\quad - \left[c(\sqrt{n} + \sqrt{\log(4m_2/\delta)}) \cdot \|\nu - \bar{\nu}\|_{\psi_2} \right] \\ &= l - 2c\sqrt{n} - c\sqrt{\log(4m_1/\delta)} \cdot \|\mu - \bar{\mu}\|_{\psi_2} \\ &\quad - c\sqrt{\log(4m_2/\delta)} \cdot \|\nu - \bar{\nu}\|_{\psi_2}, \end{aligned}$$

where the first inequality holds due to the triangle inequality. The second inequality holds due to (9) and (10).

For $\max_{i,j} \|X_i - Y_j - \bar{X}_i + \bar{Y}_j\|_2$, we have

$$\begin{aligned} \max_{i,j} \|X_i - Y_j - \bar{X}_i + \bar{Y}_j\|_2 &\leq \max_{i,j} \|X_i - \bar{\mu}\|_2 + \|Y_j - \bar{\nu}\|_2 \\ &\quad + \|\bar{X}_i - \bar{\mu}\|_2 + \|\bar{Y}_j - \bar{\nu}\|_2 \\ &\leq \left[c(\sqrt{n} + \sqrt{\log(4m_1/\delta)}) \cdot \|\mu - \bar{\mu}\|_{\psi_2} \right] + \left[c(\sqrt{n} + \sqrt{\log(4m_2/\delta)}) \cdot \|\nu - \bar{\nu}\|_{\psi_2} \right] \\ &\quad + \left[c' \frac{\sqrt{n} + \sqrt{\log(1/\delta)}}{\sqrt{m_1}} \|\mu - \bar{\mu}\|_{\psi_2} \right] + \left[c' \frac{\sqrt{d} + \sqrt{\log(1/\delta)}}{\sqrt{m_2}} \|\nu - \bar{\nu}\|_{\psi_2} \right] \\ &\leq C\sqrt{n} \left[1 + \frac{\|\mu - \bar{\mu}\|_{\psi_2}}{\sqrt{m_1}} + \frac{\|\nu - \bar{\nu}\|_{\psi_2}}{\sqrt{m_2}} \right] \\ &\quad + C \left[\sqrt{\log(4m_1/\delta)} \cdot \|\mu - \bar{\mu}\|_{\psi_2} + \sqrt{\log(4m_2/\delta)} \cdot \|\nu - \bar{\nu}\|_{\psi_2} \right], \end{aligned}$$

where the first inequality holds due to (9), (10), (11) and (12). Therefore, we have the following conclusion: As long as

$$\begin{aligned} l &\geq C\sqrt{n} \left[1 + \|\mu - \bar{\mu}\|_{\psi_2} + \|\nu - \bar{\nu}\|_{\psi_2} \right] \\ &\quad + C \left[\sqrt{\log(4m_1/\delta)} \cdot \|\mu - \bar{\mu}\|_{\psi_2} + \sqrt{\log(4m_2/\delta)} \cdot \|\nu - \bar{\nu}\|_{\psi_2} \right], \end{aligned}$$

where C is an absolute constant, we can conclude that

$$\max_{i,j} \|X_i - Y_j - \bar{X}_i + \bar{Y}_j\|_2 \leq \max_{i,j} \|X_i - Y_j\|_2.$$

This completes the proof of Theorem 4. \square

C.2 High Dimensional Probability Basics

In this section, we introduce some basic knowledge we will use in the proof of Theorem. The results mostly come from Vershynin [2018].

We first introduce a broad and widely used distribution class.

Definition 5 (Sub-Gaussian). *A random variable X that satisfies one of the following equivalent properties is called a subgaussian random variable.*

(a) *There exists $K_1 > 0$ such that the tails of X satisfy*

$$\mathbb{P}\{|X| \geq t\} \leq 2 \exp(-t^2/K_1^2) \text{ for all } t \geq 0.$$

(b) *There exists $K_2 > 0$ such that the moments of X satisfy*

$$\|X\|_{L^p} = (\mathbb{E}|X|^p)^{1/p} \leq K_2\sqrt{p} \text{ for all } p \geq 1.$$

(c) There exists $K_3 > 0$ such that the moment-generating function (MGF) of X^2 satisfies

$$\mathbb{E} \exp(\lambda^2 X^2) \leq \exp(K_3^2 \lambda^2) \text{ for all } \lambda \text{ such that } |\lambda| \leq \frac{1}{K_3}.$$

(d) There exists $K_4 > 0$ such that the MGF of X^2 is bounded at some point, namely,

$$\mathbb{E} \exp(X^2/K_4^2) \leq 2.$$

(e) Moreover, if $\mathbb{E}X = 0$, the following property is also equivalent. There exists $K_5 > 0$ such that the MGF of X satisfies

$$\mathbb{E} \exp(\lambda X) \leq \exp(K_5^2 \lambda^2) \text{ for all } \lambda \in \mathbb{R}.$$

The parameters $K_i > 0$ appearing in these properties differ from each other by at most an absolute constant factor.

The sub-Gaussian norm of X , denoted $\|X\|_{\psi_2}$, is defined to be

$$\|X\|_{\psi_2} = \inf\{t > 0 : \mathbb{E} \exp(X^2/t^2) \leq 2\}.$$

Definition 6. A random vector $X \in \mathbb{R}^d$ is sub-Gaussian if for any vector $\mathbf{u} \in \mathbb{R}^d$ the inner product $\langle X, \mathbf{u} \rangle$ is a sub-Gaussian random variable. And the corresponding ψ_2 norm of X is defined as

$$\|X\|_{\psi_2} = \sup_{\|\mathbf{u}\|_2=1} \|\langle X, \mathbf{u} \rangle\|_{\psi_2}.$$

Theorem 5. Let $X_1, \dots, X_N \in \mathbb{R}^d$ be independent, mean zero, sub-Gaussian random vectors. Then $\sum_{i=1}^N X_i$ is also a sub-Gaussian random vector, and

$$\left\| \sum_{i=1}^N X_i \right\|_{\psi_2}^2 \leq C \sum_{i=1}^N \|X_i\|_{\psi_2}^2.$$

where C is an absolute constant.

Proof of Theorem 5. For any vector $\mathbf{u} \in \mathbb{R}^d$, $\|\mathbf{u}\|_2 = 1$, consider $\langle \sum_{i=1}^N X_i, \mathbf{u} \rangle$. Using independence, we have for all λ ,

$$\begin{aligned} \mathbb{E} \exp\left(\lambda \sum_{i=1}^N \langle X_i, \mathbf{u} \rangle\right) &= \prod_{i=1}^N \mathbb{E} \exp(\lambda \langle X_i, \mathbf{u} \rangle) \\ &\leq \prod_{i=1}^N \exp(C \|\langle X_i, \mathbf{u} \rangle\|_{\psi_2}^2 \lambda^2) \\ &= \exp\left(C \lambda^2 \sum_{i=1}^N \|\langle X_i, \mathbf{u} \rangle\|_{\psi_2}^2\right), \end{aligned}$$

where C is an absolute constant and the first inequality holds due to property (e) of the sub-Gaussian variables. Taking supreme over \mathbf{u} , we prove that $\sum_{i=1}^N X_i$ is also a sub-Gaussian random vector. Moreover,

$$\left\| \sum_{i=1}^N X_i \right\|_{\psi_2}^2 \leq C \sum_{i=1}^N \|X_i\|_{\psi_2}^2.$$

where C is an absolute constant. □

Theorem 6. Let $X \in \mathbb{R}^d$ be a sub-Gaussian random vector. Then with probability at least $1 - \delta$,

$$\|X\|_2 \leq c(\sqrt{d} + \sqrt{\log(1/\delta)}) \cdot \|X\|_{\psi_2}.$$

Proof. Let B_d be the d -dimensional unit ball, N be a $1/2$ -covering of B_d in 2-norm with covering number $= N(B_d, \|\cdot\|_2, 1/2)$. Therefore,

$$\forall \mathbf{x} \in B_d, \exists \mathbf{z} \in N, \text{ s.t. } \|\mathbf{x} - \mathbf{z}\| \leq 1/2.$$

Using Lemma 1, we have

$$N \leq 5^d. \tag{13}$$

Using the fact $\|\mathbf{x}\|_2 = \max_{\|\mathbf{y}\|_2 \leq 1} \langle \mathbf{x}, \mathbf{y} \rangle$, we have

$$\begin{aligned} \|X\|_2 &= \max_{\mathbf{x} \in B_d} \langle \mathbf{x}, X \rangle \\ &\leq \max_{\mathbf{z} \in N} \langle \mathbf{z}, X \rangle + \max_{\mathbf{y} \in (1/2)B_d} \langle \mathbf{y}, X \rangle \\ &= \max_{\mathbf{z} \in N} \langle \mathbf{z}, X \rangle + \frac{1}{2} \max_{\mathbf{y} \in B_d} \langle \mathbf{y}, X \rangle. \end{aligned}$$

Therefore, we have

$$\|X\|_2 \leq 2 \max_{\mathbf{z} \in N} \langle \mathbf{z}, X \rangle. \tag{14}$$

Then we can provide a high probability upper bound for the Euclidean norm of the random vector X by considering the probability $\mathbb{P}(\|X\|_2 \geq t)$.

$$\begin{aligned} \mathbb{P}(\|X\|_2 \geq t) &\leq \mathbb{P}\left(\max_{\mathbf{z} \in N} \langle \mathbf{z}, X \rangle \geq \frac{t}{2}\right) \\ &\leq \mathbb{P}\left(\exists \mathbf{z} \in N, \langle \mathbf{z}, X \rangle \geq \frac{t}{2}\right) \\ &\leq \sum_{\mathbf{z} \in N} \mathbb{P}\left(\langle \mathbf{z}, X \rangle \geq \frac{t}{2}\right) \\ &\leq N \exp\left(-c \frac{t^2}{\|X\|_{\psi_2}^2}\right) \\ &\leq 5^d \exp\left(-\frac{ct^2}{\|X\|_{\psi_2}^2}\right), \end{aligned}$$

where c is an absolute constant. Here the first inequality holds due to (14). The second inequality holds due to $\{\max_{\mathbf{z} \in N} \langle \mathbf{z}, X \rangle \geq t/2\} \subseteq \{\exists \mathbf{z} \in N, \langle \mathbf{z}, X \rangle \geq t/2\}$. The third inequality holds due to the union bound. The fourth inequality holds due to the definition of the sub-Gaussian vector and the property (a) of a sub-Gaussian variable. The last inequality holds due to (13).

Finally, let $t = \sqrt{[d \log 5 + \log(1/\delta)]/c} \cdot \|X\|_{\psi_2}$. We have with probability at least $1 - \delta$,

$$\|X\|_2 \geq t.$$

Finally, using $\sqrt{a+b} \leq \sqrt{a} + \sqrt{b}$, we complete the proof of Theorem 6. \square

Definition 7 (ϵ -covering). *Let $(V, \|\cdot\|)$ be a normed space, and $\Theta \subset V$. V_1, \dots, V_N is an ϵ -covering of Θ if $\Theta \subseteq \cup_{i=1}^N V_i$, or equivalently, $\forall \theta \in \Theta, \exists i$ such that $\|\theta - V_i\| \leq \epsilon$.*

Definition 8 (Covering number). *The covering number is defined by*

$$N(\Theta, \|\cdot\|, \epsilon) := \min\{n : \exists \epsilon\text{-covering over } \Theta \text{ of size } n\}.$$

Lemma 1. *Let B_d be the d -dimensional Euclidean unit ball. Consider $N(B_d, \|\cdot\|_2, \epsilon)$. When $\epsilon \geq 1$, $N(B_d, \|\cdot\|_2, \epsilon) = 1$. When $\epsilon < 1$, we have*

$$\left(\frac{1}{\epsilon}\right)^d \leq N(B_d, \|\cdot\|_2, \epsilon) \leq \left(1 + \frac{2}{\epsilon}\right)^d.$$